

Human TMPRSS2 non-catalytic ectodomain and SARS-CoV-2 S2' subunit interaction mediated SARS-CoV-2 endocytosis: A model proposal with virtual screening for potential drug molecules to inhibit this interaction

Guruprasad Varma Konduru

Centre for DNA Fingerprinting and Diagnostics

Hampapathalu Adimurthy Nagarajaram (✉ hansl@uohyd.ac.in)

Department of Systems and Computational Biology, School of Life Sciences, University of Hyderabad <https://orcid.org/0000-0001-8568-0620>

Research Article

Keywords: COVID-19, humanTMPRSS2, Spike S2', Virtual Screening, Protein-Protein docking, drug repurposing, endocytosis of SARS-CoV-2

Posted Date: April 14th, 2022

DOI: <https://doi.org/10.21203/rs.3.rs-1552691/v1>

License: © ⓘ This work is licensed under a Creative Commons Attribution 4.0 International License. [Read Full License](#)

Abstract

This study proposes a novel model for SARS-CoV-2 viral integration into the host cell via endocytosis pathway and hence a target for preventive treatment of COVID-19 infection. SARS-CoV-2 spike protein undergoes proteolytic cleavage at S1-S2 cleavage site and the cleaved out S2 domain is further cleaved by the activated serine protease domain of humanTMPRSS2 to become S2'. The activated serine protease domain of TMPRSS2 is formed after it undergoes autocatalysis by which the catalytic domain is cleaved from the membrane bound non-catalytic ectodomain (hNECD) comprising of LDLRA CLASS-I repeat and a SRCR domain. It is known that the SRCR domains as well as LDLRA repeat harboring proteins mediate endocytosis of viruses and certain ligands. Based on this, we put forward a hypothesis that the exposed hNECD binds to the S2' as both are at an interaction proximity soon after S2' is processed by the serine protease domain and this interaction may lead to the endocytosis of virus as an alternate mechanism to the direct fusion model. Based on this hypothesis we have modelled the hNECD structure, followed by protein-protein docking studies with the known 3D structure of S2'. The interaction interface of hNECD discerned from the modelled complex structure was used for virtual screening of known FDA-approved drug molecules and also some of the Indian medicinal plant-based compounds. We also mapped the known mutations of concern and mutations of interest on interaction interface of S2' and found that none of the known mutations map onto the interaction interface. This indicates that targeting the probable interaction between the hNECD of TMPRSS2 and S2' may serve as an attractive potential therapeutic target which is variant independent.

Introduction

COVID-19 caused by SARS-CoV2, within a few months of its first report quickly attained a pandemic status globally leading to the unprecedented loss of many human lives. In addition, many countries have been severely impacted social-economically due to the impending lock-downs to contain the spread of the virus. With the recent emergence of Omicron variant of SARS-CoV2, there is a general expectation among the medical fraternity that some other variants of concern may emerge, some of which may perhaps be more contagious than the previous variants, with a potential to infect people including those vaccinated as well as the ones having a previous history of COVID-19. Hence, there is a need to investigate the virus biology in the host much more deeply than what has been done already and this can give rise to novel targets for drug design or for repurposing of known drugs to prevent or to treat SARS-CoV2 infections.

Hitherto, studies toward the development of antiviral compounds against COVID-19 have focused on some of the human as well as viral factors as targets as these have been found to play key roles during different stages of life cycle of the virus (Liu et al., 2020). Among the targets, the host factor human TMPRSS2 has been shown to facilitate viral infection by means of two independently carried out functions: a) Priming of the viral Spike protein (S-protein) leading to the generation of the fusion peptide referred to as S2' (Heurich et al., 2014) and b) proteolytic cleavage of the ACE2 receptor after it binds to the cleaved S1 subunit of the viral Spike protein (Hoffmann et al., 2020).

HumanTMPRSS2 is a membrane-bound serine protease of 492 aa length and it is composed of the cytosolic part (1–84), the transmembrane part (85–105) and the ectodomain (106–492). The ectodomain further is composed of the N-terminal part comprising of one 38 aa long Low Density Lipid Receptor- Class A (LDLRA) repeat (112–149) and one 93 aa long Scavenger Receptor Cysteine Rich Domain (SRCRD) (150–242) and the C-terminal part comprising of one 234 aa long Serine protease Domain (SPD) (Fig. 1). Henceforth, for convenience, we refer to the N-terminal non-serine protease part of the ectodomain of human TMPRSS2 as hNECD. It has been shown that the human TMPRSS2 undergoes autocleavage in prostate cancer cells expressing TMPRSS2 by which the SPD cleaves out of the whole protein leaving behind the membrane bound hNECD (Afar et al., 2001). Recently, a study has also asserted and confirmed the cleavage of the catalytic domain from the hNECD (preprint Fraser et al., 2021).

SRCRD of hNECD belongs to the superfamily of SRCR domains found only in eukaryotes. These domains are highly conserved and found in many cell receptors (Sarras et al., 2004). SRCRs have been known to bind to different types of ligands including LDLs, bacteria, viruses and even mediate their endocytosis (Kaksonen & Roux, 2018; Yap, Whelan, Bowdish, & Golding, 2015). SRCR domains have been reported to be essential for infection of pigs by porcine reproductive and respiratory syndrome virus (PRRSV). Gene knockout of a specific SRCR5 domain in pigs made them resistant to PRRSV1 virus (Burkard et al., 2018). The LDLRAs are also known to be part of proteins involved in the endocytic pathway (<https://prosite.expasy.org/doc/PS01209>). LDLR receptors have been reported to be the host cell attachment receptors for Human Rhinovirus 2(HRV2), followed by their entry into host cells mediated by clathrin-mediated endocytosis (Fuchs & Blaas, 2012).

Using the above information as basis we wish to put forward a hypothesis that the membrane bound exposed hNECD may bind to S2' soon after cleavage by the activated serine protease of TMPRSS2 and this interaction may mediate the endocytosis of virus particles into the human cell (Fig. 2). We further propose a model for this interaction and virtually screen for the known set of approved drugs and known phytochemicals that might disrupt the interaction of hNECD with S2'. This we believe might open a new paradigm on the virus entry into the host that also helps development of a new treatment regime for COVID-19. Besides this, we observe that none of the known mutations of concern and mutations of interest map on to the interaction interface of the S2' with hNECD and therefore, any drug development toward disruption of this interaction, can potentially give rise to a variant-independent treatment regime.

Methodology

Modelling of hNECD 3D-structure

X-ray/NMR/Cryo structure of hNECD is not yet available, and therefore we used AlphaFold V2.1.0 (Jumper et al., 2021) google collab server (<https://colab.research.google.com/github/deepmind/alphafold/blob/main/notebooks/AlphaFold.ipynb>) to model the 3D structure of hNECD based on its protein sequence. We selected the best model (Fig. 3) among five predicted models and further validated for its stereochemical quality and fold compatibility using PROCHECK (R. A. Laskowski, MacArthur, Moss, & Thornton, 1993) and Errat plot (Colovos & Yeates, 1993) respectively.

SARS-CoV-2 spike protein

Many crystal structures of spike protein of SARS-CoV-2 have been solved, and among them, many have gap regions in the S2' structure. Among these, we chose the Cryo-EM structure representing a prefusion state (PDB id:6XR8) (Cai et al., 2020) as it has the complete S2' fusion peptide region. Spike protein is in homo-trimer structure, and as per initial evidence, spike protein cleaved at the second cleavage site before fusion with the human cell membrane, and this state is referred to as a prefusion state. We removed the amino acid residues till the second cleavage site in the S2 region (till R815) using PyMol2.3.4 (Schrodinger, LLC), and we labeled the remaining structure with residues (S816-P1162) as VS2' (Fig. 1) and used this structure for the protein-protein docking and simulation studies as detailed below.

Protein-Protein docking studies

We used Haddock2.2 (Van Zundert et al., 2016) server (<https://wenmr.science.uu.nl/haddock2.4/>) for protein-protein docking studies. We used the modelled hNECD structure and the VS2' structure as input structures and performed a blind docking considering the entire structure of modelled hNECD and residues in range (816–883 and 948–1029) in VS2' for sampling along with the default HADDOCK docking parameters for protein-protein docking. PPCheck protein-protein interaction tool (Sukhwai & Sowdhamini, 2013) was used to analyze the different docking poses for their binding energies, presence of salt-bridges and hydrogen bonds at protein-protein interaction interface.

MD Simulations of hNECD and VS2' complex

MD simulations were used to ascertain the stability of the complex and were carried out using Gromacs version 2020.5 (Abraham et al., 2015; Lindahl, Hess, & van der Spoel, 2020). The OPLS-AA force field was used with TIP3P water model (MacKerell Jr et al., 1998) for solvation of periodic boundary conditions of 1.0 nm. We used steepest descent minimization algorithm for energy minimization of the hNECD-VS2' complex structure. The energy minimum structure so obtained was subjected to MD simulations first by NVT followed by NPT protocols. We used a modified Berendsen thermostat (Berendsen et al. 1984) to maintain constant temperature and Parrinello-Rahman barostat algorithm (Nosé & Klein, 1983; Parrinello & Rahman, 1981) to maintain constant pressure during the simulations. We carried out MD simulations for 100ns by constraining backbone of VS2' in hNECD-VS2' complex.

We used the gmx tool gmx_rmsd to analyze RMSD and gmx_distance to calculate the distance between atoms forming salt bridge interactions. VMD 1.9.3 (Humphrey, Dalke, & Schulten, 1996) extensions Salt Bridges and Hydrogens Bonds were used to calculate salt bridge interactions and hydrogen bond interactions throughout simulations. We clustered the time frames obtained during the simulation using gmx cluster with rmsd cutoff of 0.2 nm. Stable cluster centroid was analyzed for hydrogen bonds, salt bridges and interface residues using PPCheck protein-protein interaction tool. We also identified the hotspot residues, which are critical for the interaction of hNECD with VS2' using the PPCheck hotspot prediction tool (Sukhwai & Sowdhamini, 2013).

Virtual screening studies

We choose the hNECD interaction surface for virtual screening using two different sets: (a) a set of US FDA-approved compounds (FDAC) and (b) a set of phytochemicals (PHTC). A set of comprising of 2186 FDACs was extracted from DRUGBANK (Wishart et al., 2006) in SDF format and its library was formed using the Open Babel (O'Boyle et al., 2011) in PDBQT format. The second set of 478 druggable phytochemical compounds in PDBQT format was extracted from the Indian medicinal plants reported in the IMPPAT database (Mohanraj et al., 2018). Autodock tools (Morris & Huey, 2009) were used to prepare hNECD for virtual screening. The search grid box was chosen such that it covers the entire interaction surface of hNECD. A shell script provided by Vina authors was used to run Autodock Vina (Trott and Arthur J. Olson, 2010) for virtual high throughput screening of the library of FDA-approved drug molecules and phytochemical compounds from Indian medicinal plants and identified 10 high scoring molecules from each set. PyMol (Schrodinger, LLC) and LigPlot+ (Roman A. Laskowski & Swindells, 2011) were used to analyse and visualize interactions between hNECD and the top scoring drug molecules.

Results

Modelling of hNECD 3D structure

As mentioned already, 3D structure of the hNECD is not yet available and therefore we built a model using AlphaFold v2.1.0 google collab server based on hNECD protein sequence (please see Fig. 3). The hNECD domain of TMPRSS2 harbors the LDLRA and SRCR domains each harboring six and four Cys residues respectively. These Cys residues in the known structures form disulfide bonds which offer stability to their structures. In the predicted hNECD model too, we observed that these S-S bonds are retained with known connections and topologies. Both the Ramachandran and ERRAT plots reveal that the model is satisfactory (supplementary Figure S1 and Figure S2 respectively).

Protein-protein docking studies

As already mentioned, we hypothesize that VS2' binds to hNECD soon after it is cleaved by the activated serine protease and this interaction might mediate the endocytosis of the virus. We, therefore, carried out docking studies on hNECD and VS2' structures and identified the best binding pose that corresponds to the lowest binding energy (-385.46 Kcal/mol) as a putative representation of the interaction between hNECD and VS2'.

hNECD-VS2' complex is stable throughout MD Simulations

We performed MD simulations of the hNECD-VS2' complex for 100ns and observed that the system stabilizes with RMSD between 0.1 to 0.2 nm, as shown in supplementary Figure S3. The interaction between hNECD and VS2' is stabilized by several H-bonds and salt-bridges. Among these the H-bonds R1000 of hNECD to D203 of VS2' and K112 of hNECD to D867 of VS2' are highly conserved during the period of simulation (present in more than 60% of frames). Among the salt bridges, E990 (VS2')-K234 (hNECD) and D867 (VS2')-K112 (hNECD) are found in 24.70% and 95.15% of time points respectively. We did clustering of instantaneous structures saved at every 10 ps with an RMSD cutoff of 0.2 nm and obtained 7 clusters. The largest cluster has 5596 snapshots with RMSD of 0.186 nm and we selected the center snapshot of this cluster as the representative of stable hNECD-VS2' complex and used this structure for virtual screening of drugs. This interaction is characterized by a number of polar and apolar interactions whose list is given in supplementary Table 1 and the list of interface residues for both the molecules is given in supplementary Table 2. hNECD interface consists of 24% charged and 53% hydrophobic amino acids and VS2' interface consists of 18% charged and 64% hydrophobic amino acids. Among interaction interface residues, PPCheck hotspot prediction tool (Sukhwai & Sowdhamini, 2013) predicted K112, R150, G153, P154, F156 of hNECD and F833, 836Q, 837Y, 864L of VS2' as hotspot residues.

It has been reported that a pair of Aspartate residues in the SRCR domain of CD163 protein binds to basic residues in its binding partner (haptoglobin-hemoglobin) (Nielsen, Andersen, & Moestrup, 2013). In our model too, we find salt bridge interactions between D203 of SRCR domain of hNECD and R1000 of VS2'.

Virtual screening of FDA approved drugs

We did the virtual screening of FDA-approved drugs that potentially bind to the hNECD binding interface (Fig. 5) using the Autodock Vina tool as mentioned in the methods section. We selected Top10 FDA approved drugs based on their docking score and their list is given in Table 1. These molecules bind to the binding pocket in hNECD and hence mask the residues 118I, 129P, 132W, 147R, 149V, 151L, 161Y, 166K, 168W, 188M and 190Y including the hotspot residues 150R, 154P and 156F at the binding interface for VS2'. Hence, these molecules have the potential to prevent interaction of VS2' with hNECD.

Table 1
List of top10 FDA approved drug molecules from virtual screening of FDA approved drugs targeting hNECD interaction interface with VS2'

Drug Bank ID	Binding Affinity (kcal/mol)	Drug name
DB09027	-11.377	Ledipasvir
DB09296	-10.8446	Ombitasvir
DB06785	-10.561	Ganirelix
DB01601	-10.117	Lopinavir
DB06287	-9.975	Temsirolimus
DB04835	-9.748	Maraviroc
DB09114	-9.716	Colfosceril palmitate
DB09374	-9.604	Indocyanine
DB11855	-9.489	Revefenacin
DB01226	-9.444	Mivacurium

Among the top molecules Ledipasvir and Ombitasvir are the known inhibitors of NS5A protein in Hepatitis C Virus (HCV). Ganirelix is an inhibitor of GnRH receptors. Lopinavir is an inhibitor of HIV-1 protease. Temsirolimus is an mTOR inhibitor used in renal cell carcinoma (RCC) treatment. Maraviroc is a CCR5 co-receptor antagonist and blocks the HIV virus entering the host cells. Colfosceril palmitate is used in the treatment of Respiratory Distress Syndrome (RDS) in premature infants. Mivacurium is a muscle relaxant. Dutasteride is an inhibitor of 5-alpha reductase and is used for the treatment of symptomatic benign prostatic hyperplasia (BPH) (Wishart et al., 2006).

It is interesting to note that among these top hits, Dutasteride has undergone clinical trials for treatment of mild COVID-19 symptoms with males. As compared to placebo treatment with this drug has shown a reduction in the duration of the disease accompanied by a reduction in fatigue (Cadejani, McCoy, Gustavo Wambier, & Goren, 2021). The clinical trials on Sofosbuvir/Ledipasvir and Lopinavir-Ritonavir combinations on a small number of COVID-19 patients have not shown significant benefits (Cao et al., 2020; Nourian et al., 2020).

Virtual screening of Phytochemical compounds

We also performed virtual screening of phytochemical compounds from Indian medicinal plants targeting the hNECD binding interface (Fig. 6). Top10 phytochemical compounds were selected based on their docking score and their list is given in Table 2. Among the top10 phytochemicals, five are from Gamhar (Gmelina Arborea) and this plant was part of a 15 herbal ingredients in the Government of India's Ayush formulation called "Agasthaya hareetaki" recommended for the management of respiratory infections (Ahmad et al., 2021). These phytochemical compounds bind at binding pocket of hNECD and masks the residues 118I, 129P, 132W, 147R, 149V, 151L, 161Y, 168W, 188M and 190Y including the hotspot residue 150R at the binding interface for VS'. As found in the case of FDA approved drugs, these phytochemicals too mask the interaction of VS2' with hNECD. Figure 6 shows the binding of the top scoring phytochemical Isoarboreol from the Gamhar medicinal plant with hNECD.

Table 2

List of top10 phytochemical compounds from virtual screening of phytochemical compounds targeting hNECD interaction interface with VS2'

Phytochemical Compound	Binding Affinity (kcal/mol)	Medicinal plant common name	Medicinal plant scientific name
PAMOIC ACID	-8.103	Periwinkle	Catharanthus roseus
Isoarboreol	-7.976	Gamhar	Gmelina arborea
4-Hydroxysesamin	-7.685	Gamhar	Gmelina arborea
Alloyohimbine	-7.602	Sarpagandha	Rauwolfia serpentina
Paulownin	-7.574	Gamhar	Gmelina arborea
Gummadiol	-7.549	Gamhar	Gmelina arborea
kaempferol 3-O-beta-D-glucoside	-7.544	Sita Ashok	Saraca asoca
I-asarinin	-7.504	Dalmatian Chrysanthemum;;Ginkgo ;Chameleon Plant;Magnolia;Tailed Pepper;Long Pepper;;Sesame;;Winged Prickly Ash	
4,8-Dihydroxysesamin	-7.486	Gamhar	Gmelina arborea
Cathenamine	-7.467	Periwinkle	Catharanthus roseus

Discussion

SARS-CoV-2 entry into the host cells has been reported to follow a direct fusion mechanism soon after the cleavage at the second cleavage site in the spike protein by the activated protease of TMPRSS2 (Wang & Xiang, 2020). Despite this, literature evidences suggest that endocytosis pathway for viral entry cannot be completely ruled out (Burkard et al., 2018; Yap et al., 2015). Taking cue from the fact that S2' cleavage by the activated serine protease domain which is tethered to the hNECD by a disulfide bond between Cys244 And Cys365, positions the hNECD and the primed VS2' at a distance proximal enough for their possible binding with each other. Our modelling followed by docking studies presented in this communication are the attempts toward giving a model of this possible interaction. We propose that the hNECD binds to primed Spike protein and results in SRCR/LDLRA domain mediated endocytosis of SARS-CoV-2 into the host cells. Till now, protein-protein Interaction between the serine protease domain of TMPRSS2 and spike protein has only been investigated to understand their molecular interactions involved in the cleavage of spike protein at S1/S2 and S2 cleavage sites (Mushtaq Hussain et al., 2020). However, the interaction between hNECD and VS2' has not yet been captured or reported. This may perhaps be due to the inability of the methods, i.e., affinity-purification mass spectrometry, to detect the interactions involving membrane-bound proteins (Gordon et al., 2020)

We have used interaction interface of hNECD from hNECD-VS2' complex for virtual screening of FDA approved drugs and druggable phytochemical compounds derived from Indian medicinal plants database and identified top10 potential drugs and top10 potential phytochemical compounds that could inhibit the interaction between hNECD and VS2' and thereby SARS-CoV-2 virus entry mediated by hNECD into host cells. We mapped known mutations of concern and mutations of interest in SARS-CoV-2 spike protein and observed none of these mutations mapped at interaction interface of VS2' with hNECD and therefore we can consider this hNECD-VS2' interaction as a potential therapeutic target for targeting the current SARS-CoV-2 variant of concerns.

Our virtual screening of FDA approved drugs has identified Dutasteride as one of the hits. This drug has undergone a clinical trial for males with mild COVID-19 symptoms with a promising benefit (Cadejani, McCoy, Gustavo Wambier, & Goren, 2021). Maraviroc which is known to block HIV entry into the host cells has also been shown by *in vitro* studies to inhibit early infection of SARS-CoV-2 (preprint Kenneth et al., 2020). In the light of our model, further studies could be carried to investigate the efficacy of these drugs in patients with COVID-19. Our studies have also identified some phytochemical compounds to initiate target i.e. hNECD-VS2' interaction-based studies. It is known that the medicinal plant Gamhar shows antiviral activity however its active compound and its possible target have not been well studied and in this light, our study can be used as the testable hypothesis to conduct further studies to check efficacy of these phytochemical compounds for the treatment of COVID-19.

Mapping of known mutations of concern and mutations of interest onto the interaction interface of S2'

Mutations with evidence of increasing transmissibility or virulence or decreasing therapeutic/vaccine efficacy are classified as Mutations of Concern (MC), and the mutations suspected of causing a change in transmissibility or virulence or therapeutic/vaccine efficacy are classified as Mutations of Interest (MI) (<https://outbreak.info/situation-reports>).

Mutation E484K has been classified as an MC and the mutations L18F, K417N, K417T, N439K, L452R, S477N, S494P, N501Y, P681H, P681R have been classified as MIs. It is interesting to find that none of these mutations (both MC and Mis) map on to the interaction interface of S2' and hNECD.

Delta variant has one mutation D950N in the S2' region and this mutation is not present at interaction interface of S2' with hNECD. Omicron strain has four mutations N856K, Q954H, N969K, and L981F in the S2' region. Out of these four mutations, two mutations N856K and L981F are at the interaction interface of S2' with hNECD. Stealth Omicron (BA.2) has only two mutations Q954H and N969K, in the S2 region and none of these mutations are at the interaction interface of S2' with hNECD. Mutations mapped on spike protein corresponding to the variants of concern are listed in the Table 3.

Table 3: Five Variants of concern SARS-CoV-2 strains and their respective mutations.

Variant of concern	Mutations in spike protein	Mutations at the interaction interface of S2'
Delta	T19R, E156G, DEL157/158, L452R, T478K, D614G, P681R, D950N	NA
Omicron	A67V, DEL69/70, T95I, G142D, DEL143/145, N211I, DEL212/212, G339D, S371L, S373P, S375F, S477N, T478K, E484A, Q493R, N501Y, Y505H, T547K, D614G, H655Y, N679K, P681H, N764K, D796Y, N856K, Q954H, N969K, L981F	N856K, L981F
Alpha	DEL69/70, DEL144/144, N501Y, A570D, D614G, P681H, T716I, S982A, D1118H	S982A
Beta	D80A, D215G, DEL241/243, K417N, E484K, N501Y, D614G, A701V	NA
Gamma	L18F, T20N, P26S, D138Y, R190S, K417T, E484K, N501Y, D614G, H655Y, T1027I, V1176F	NA

It is to be noted that an attempt was made to investigate interaction between hNECD and VS2' by expressing the synthetic genes corresponding to the hNECD and VS2' in E.coli using the standard pull down assays. This study could not identify interaction between the engineered proteins (Dayananda Siddavattam, Private communication). This result could be considered as a false-negative due to the following reason. The proteins of the synthetic genes correspond to the truncated domains devoid of their membrane anchoring parts and other domains. It is very likely that these unanchored isolated proteins do not fold into the required 3D structures under the experimental conditions. Needless to mention the folded structures are quintessential for protein-protein interactions.

Declarations

Acknowledgements

KGV is a recipient of Junior research fellowship and Senior research fellowship from Council of Scientific and Industrial Research, New Delhi. KGV also acknowledge Centre for DNA Fingerprinting and Diagnostics Core fund for supporting this work. HAN acknowledges the university core

funding as well as a grant from Department of Science and Technology, New Delhi. The authors acknowledge Bioinformatics Infrastructure Facility (BIF), School of Life Sciences, University of Hyderabad. The authors gratefully acknowledge the engaging discussions with Prof. Dayananda, and the laboratory members Dr. Chhaya Singh, Mrs. Nithya, Ms. Aishwarya Gholve and Ms. Rachana.

Competing Interests

The authors declare no competing interests

References

1. Abraham, M. J., Murtola, T., Schulz, R., Páll, S., Smith, J. C., Hess, B., & Lindahl, E. (2015). GROMACS: High performance molecular simulations through multi-level parallelism from laptops to supercomputers. *SoftwareX*, *1*, 19–25.
2. Afar, D. E. H., Vivanco, I., Hubert, R. S., Kuo, J., Chen, E., Saffran, D. C., ... Jakobovits, A. (2001). Catalytic cleavage of the androgen-regulated TMPRSS2 protease results in its secretion by prostate and prostate cancer epithelia. *Cancer Research*, *61*(4), 1686–1692.
3. Ahmad, S., Zahiruddin, S., Parveen, B., Basist, P., Parveen, A., Gaurav, ... Ahmad, M. (2021). Indian Medicinal Plants and Formulations and Their Potential Against COVID-19—Preclinical and Clinical Research. *Frontiers in Pharmacology*, *11*(March). <https://doi.org/10.3389/fphar.2020.578970>
4. Berendsen, H. J. C., Postma, J. P. M., Van Gunsteren, W. F., Dinola, A., & Haak, J. R. (1984). Molecular dynamics with coupling to an external bath. *The Journal of Chemical Physics*, *81*(8), 3684–3690. <https://doi.org/10.1063/1.448118>
5. Burkard, C., Opriessnig, T., Mileham, A. J., Stadejek, T., Ait-Ali, T., Lillico, S. G., ... Archibald, A. L. (2018). Pigs Lacking the Scavenger Receptor Cysteine-Rich Domain 5 of CD163 Are Resistant to Porcine Reproductive and Respiratory Syndrome Virus 1 Infection. *Journal of Virology*, *92*(16). <https://doi.org/10.1128/jvi.00415-18>
6. Cadegiani, F. A., McCoy, J., Gustavo Wambier, C., & Goren, A. (2021). Early Antiandrogen Therapy With Dutasteride Reduces Viral Shedding, Inflammatory Responses, and Time-to-Remission in Males With COVID-19: A Randomized, Double-Blind, Placebo-Controlled Interventional Trial (EAT-DUTA AndroCoV Trial – Biochemical). *Cureus*, *13*(2), 1–13. <https://doi.org/10.7759/cureus.13047>
7. Cai, Y., Zhang, J., Xiao, T., Peng, H., Sterling, S. M., Walsh, R. M., ... Chen, B. (2020). Distinct conformational states of SARS-CoV-2 spike protein. *Science*, *369*(6511), 1586–1592. <https://doi.org/10.1126/science.abd4251>
8. Cao, B., Wang, Y., Wen, D., Liu, W., Wang, J., Fan, G., ... Wang, C. (2020). A Trial of Lopinavir–Ritonavir in Adults Hospitalized with Severe Covid-19. *New England Journal of Medicine*, *382*(19), 1787–1799. <https://doi.org/10.1056/nejmoa2001282>
9. Colovos, C., & Yeates, T. O. (1993). Verification of protein structures: Patterns of nonbonded atomic interactions. *Protein Science*, *2*(9), 1511–1519. <https://doi.org/10.1002/pro.5560020916>
10. Fraser, B. J., Beldar, S., Seitova, A., Hutchinson, A., Mannar, D., Li, Y., ... Bénard, F. (2021). Structure, activity and inhibition of human TMPRSS2, a protease implicated in SARS-CoV-2 activation. *BioRxiv*, 2021.06.23.449282. Retrieved from <https://www.biorxiv.org/content/10.1101/2021.06.23.449282v1%0Ahttps://www.biorxiv.org/content/10.1101/2021.06.23.449282v1.abstract>
11. Fuchs, R., & Blaas, D. (2012). Productive entry pathways of human rhinoviruses. *Advances in Virology*, *2012*. <https://doi.org/10.1155/2012/826301>
12. Gordon, D. E., Jang, G. M., Bouhaddou, M., Xu, J., Obernier, K., White, K. M., ... Krogan, N. J. (2020). A SARS-CoV-2 protein interaction map reveals targets for drug repurposing. *Nature*, *583*(7816), 459–468. <https://doi.org/10.1038/s41586-020-2286-9>
13. Heurich, A., Hofmann-Winkler, H., Gierer, S., Liepold, T., Jahn, O., & Pohlmann, S. (2014). TMPRSS2 and ADAM17 Cleave ACE2 Differentially and Only Proteolysis by TMPRSS2 Augments Entry Driven by the Severe Acute Respiratory Syndrome Coronavirus Spike Protein. *Journal of Virology*, *88*(2), 1293–1307. <https://doi.org/10.1128/jvi.02202-13>
14. Hoffmann, M., Kleine-Weber, H., Schroeder, S., Krüger, N., Herrler, T., Erichsen, S., ... Pöhlmann, S. (2020). SARS-CoV-2 Cell Entry Depends on ACE2 and TMPRSS2 and Is Blocked by a Clinically Proven Protease Inhibitor. *Cell*, *181*(2), 271–280.e8. <https://doi.org/10.1016/j.cell.2020.02.052>
15. Humphrey, W., Dalke, A., & Schulten, K. (1996). VMD: visual molecular dynamics. *Journal of Molecular Graphics*, *14*(1), 33–38.
16. Jumper, J., Evans, R., Pritzel, A., Green, T., Figurnov, M., Ronneberger, O., ... Hassabis, D. (2021). Highly accurate protein structure prediction with AlphaFold. *Nature*, *596*(7873), 583–589. <https://doi.org/10.1038/s41586-021-03819-2>
17. Kaksonen, M., & Roux, A. (2018). Mechanisms of clathrin-mediated endocytosis. *Nature Reviews Molecular Cell Biology*, *19*(5), 313–326. <https://doi.org/10.1038/nrm.2017.132>
18. Laskowski, R. A., MacArthur, M. W., Moss, D. S., & Thornton, J. M. (1993). PROCHECK: a program to check the stereochemical quality of protein structures. *Journal of Applied Crystallography*, *26*(2), 283–291. <https://doi.org/10.1107/S0021889892009944>
19. Laskowski, Roman A., & Swindells, M. B. (2011). LigPlot+: Multiple ligand-protein interaction diagrams for drug discovery. *Journal of Chemical Information and Modeling*, *51*(10), 2778–2786. <https://doi.org/10.1021/ci200227u>

20. Lindahl, A., Hess, S. V. der, & van der Spoel, D. (2020). *GROMACS 2020 Source code*. Zenodo.
21. Liu, C., Zhou, Q., Li, Y., Garner, L. V., Watkins, S. P., Carter, L. J., ... Albaiu, D. (2020). Research and Development on Therapeutic Agents and Vaccines for COVID-19 and Related Human Coronavirus Diseases. *ACS Central Science*, *6*(3), 315–331. <https://doi.org/10.1021/acscentsci.0c00272>
22. MacKerell Jr, A. D., Bashford, D., Bellott, M., Dunbrack Jr, R. L., Evanseck, J. D., Field, M. J., ... Ha, S. (1998). All-atom empirical potential for molecular modeling and dynamics studies of proteins. *The Journal of Physical Chemistry B*, *102*(18), 3586–3616.
23. Mohanraj, K., Karthikeyan, B. S., Vivek-Ananth, R. P., Chand, R. P. B., Aparna, S. R., Mangalapandi, P., & Samal, A. (2018). IMPPAT: A curated database of Indian Medicinal Plants, Phytochemistry and Therapeutics. *Scientific Reports*, *8*(1), 1–17. <https://doi.org/10.1038/s41598-018-22631-z>
24. Morris, G., & Huey, R. (2009). AutoDock4 and AutoDockTools4: Automated docking with selective receptor flexibility. *Journal of ...*, *30*(16), 2785–2791. <https://doi.org/10.1002/jcc.21256>.AutoDock4
25. Nielsen, M. J., Andersen, C. B. F., & Moestrup, S. K. (2013). CD163 binding to haptoglobin-hemoglobin complexes involves a dual-point electrostatic receptor-ligand pairing. *Journal of Biological Chemistry*, *288*(26), 18834–18841. <https://doi.org/10.1074/jbc.M113.471060>
26. Nosé, S., & Klein, M. L. (1983). Constant pressure molecular dynamics for molecular systems. *Molecular Physics*, *50*(5), 1055–1076.
27. Nourian, A., Khalili, H., Ahmadinejad, Z., Kouchak, H. E., Jafari, S., Manshadi, S. A. D., ... Kebriaeezadeh, A. (2020). Efficacy and safety of sofosbuvir/ ledipasvir in treatment of patients with covid-19; a randomized clinical trial. *Acta Biomedica*, *91*(4), 1–14. <https://doi.org/10.23750/abm.v91i4.10877>
28. O'Boyle, N. M., Banck, M., James, C. A., Morley, C., Vandermeersch, T., & Hutchison, G. R. (2011). Open Babel. *Journal of Cheminformatics*, *3*(33), 1–14. Retrieved from <https://jcheminf.biomedcentral.com/track/pdf/10.1186/1758-2946-3-33>
29. Parrinello, M., & Rahman, A. (1981). Polymorphic transitions in single crystals: A new molecular dynamics method. *Journal of Applied Physics*, *52*(12), 7182–7190. <https://doi.org/10.1063/1.328693>
30. Sarrias, M. R., Gronlund, J., Padilla, O., Madsen, J., Holmskov, U., & Lozano, F. (2004). The Scavenger Receptor Cysteine-Rich (SRCR) domain: an ancient and highly conserved protein module of the innate immune system. *Critical Reviews™ in Immunology*, *24*(1).
31. Sukhwal, A., & Sowdhamini, R. (2013). Oligomerisation status and evolutionary conservation of interfaces of protein structural domain superfamilies. *Molecular BioSystems*, *9*(7), 1652–1661. <https://doi.org/10.1039/c3mb25484d>
32. TROTT, O., & ARTHUR J. OLSON. (2010). Software News and Updates AutoDock Vina: Improving the Speed and Accuracy of Docking with a New Scoring Function, Efficient Optimization, and Multithreading. *Journal of Computational Chemistry*, *31*, 455–461. <https://doi.org/10.1002/jcc>
33. Van Zundert, G. C. P., Rodrigues, J. P. G. L. M., Trellet, M., Schmitz, C., Kastiris, P. L., Karaca, E., ... Bonvin, A. M. J. J. (2016). The HADDOCK2.2 Web Server: User-Friendly Integrative Modeling of Biomolecular Complexes. *Journal of Molecular Biology*, *428*(4), 720–725. <https://doi.org/10.1016/j.jmb.2015.09.014>
34. Wang, L., & Xiang, Y. (2020). Spike Glycoprotein-Mediated Entry of SARS Coronaviruses. *Viruses*, (12), 1289.
35. Wishart, D. S., Knox, C., Guo, A. C., Shrivastava, S., Hassanali, M., Stothard, P., ... Woolsey, J. (2006). DrugBank: a comprehensive resource for in silico drug discovery and exploration. *Nucleic Acids Research*, *34*(Database issue), 668–672. <https://doi.org/10.1093/nar/gkj067>
36. Yap, N. V. L., Whelan, F. J., Bowdish, D. M. E., & Golding, G. B. (2015). The evolution of the scavenger receptor cysteine-rich domain of the class A scavenger receptors. *Frontiers in Immunology*, *6*(JUN), 1–9. <https://doi.org/10.3389/fimmu.2015.00342>

Figures

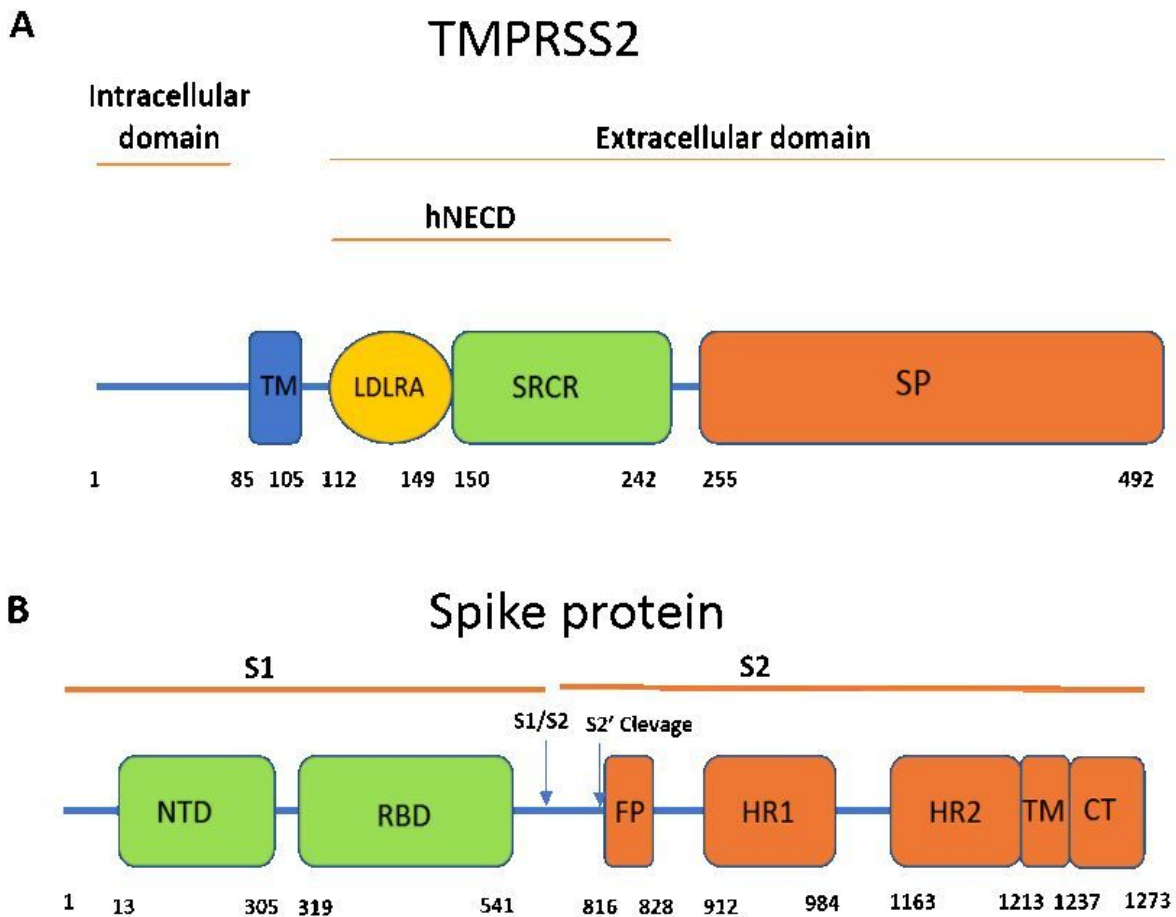


Figure 1

Schematic representation of domains present in A) human TMPRSS2 and B) SARS-CoV-2 Spike protein. Spike protein has two cleavage sites S1/S2 and S2' cleavage site.

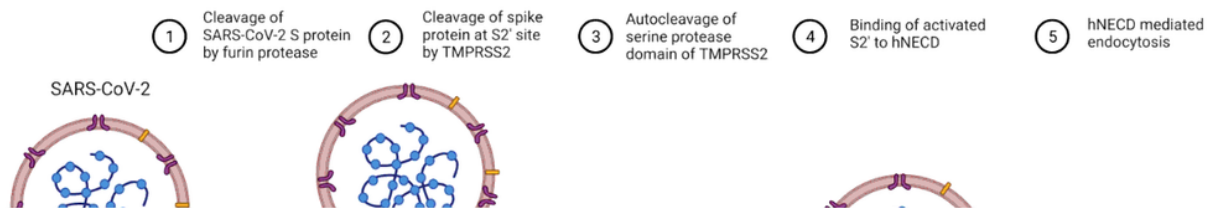


Figure 2

TMPRSS2 mediated entry of SARS-CoV-2 into host cells. (figure created using BioRender)

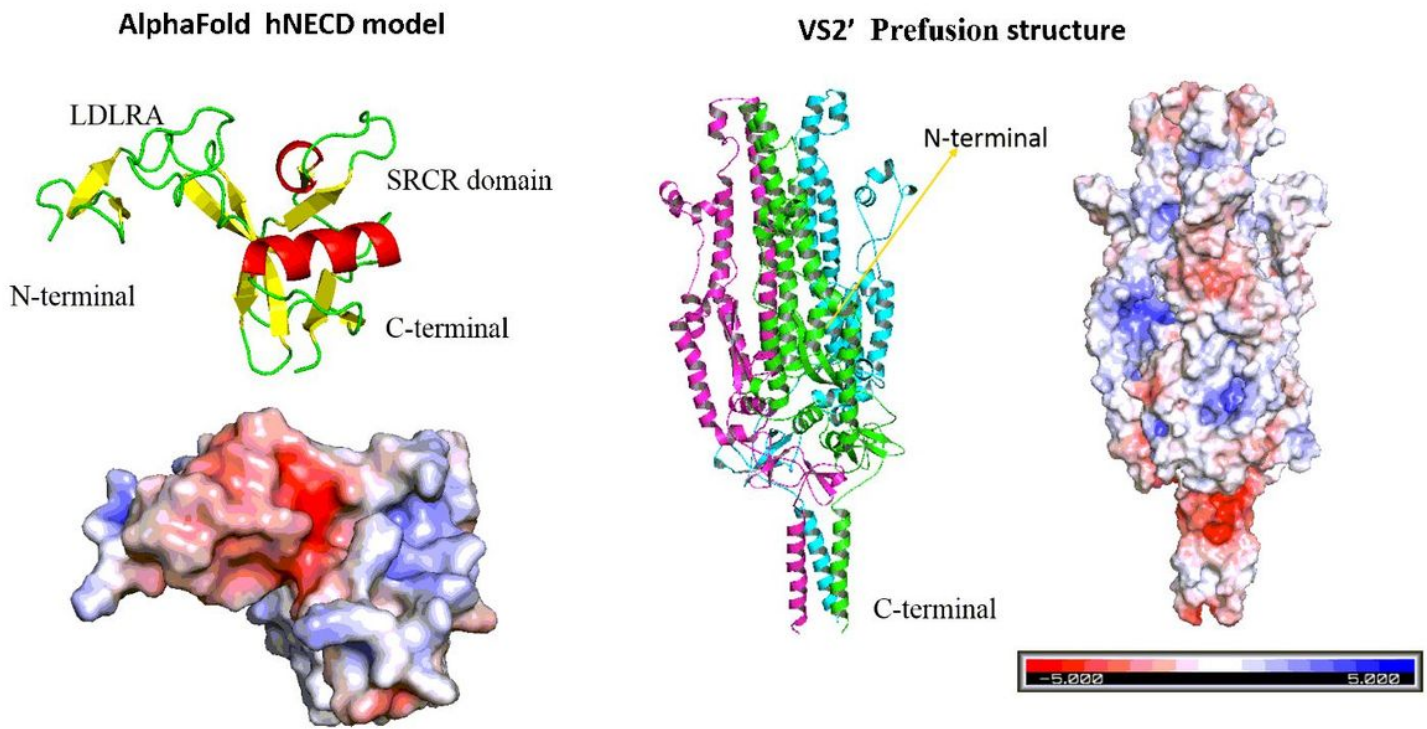


Figure 3

3D structures of AlphaFold modelled hNECD and VS2' structures (PDB Id: 6XR8) ribbon model and surface view visualized using PyMol (Schrodinger, LLC).

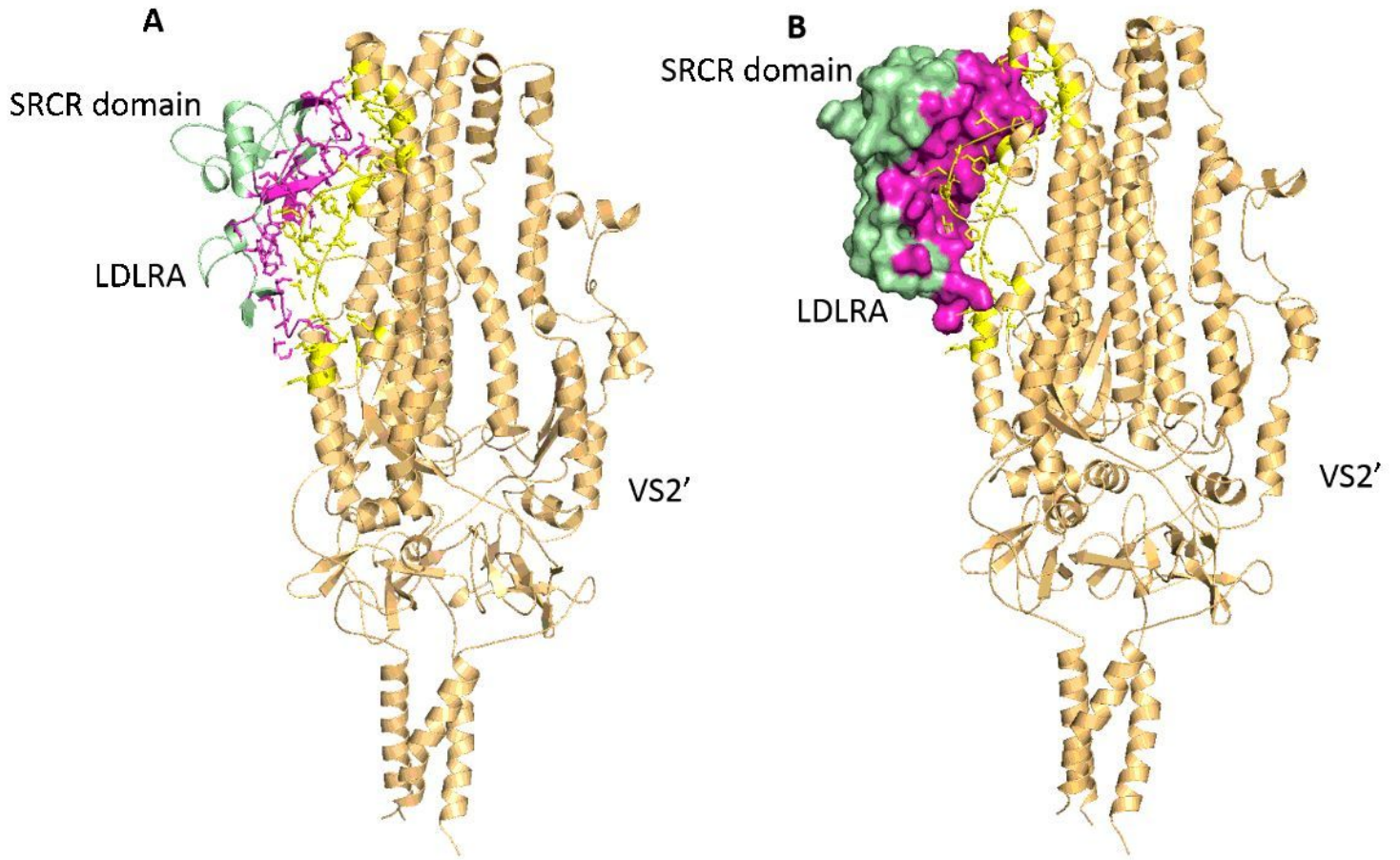


Figure 4

Stable hNECD-VS2' complex obtained after MD Simulations. hNECD interface is represented in magenta color and VS2' interface is represented in yellow color. hNECD and VS2' are represented in cartoon in panel A and panel B shows surface view of hNECD and cartoon representation of VS2'.

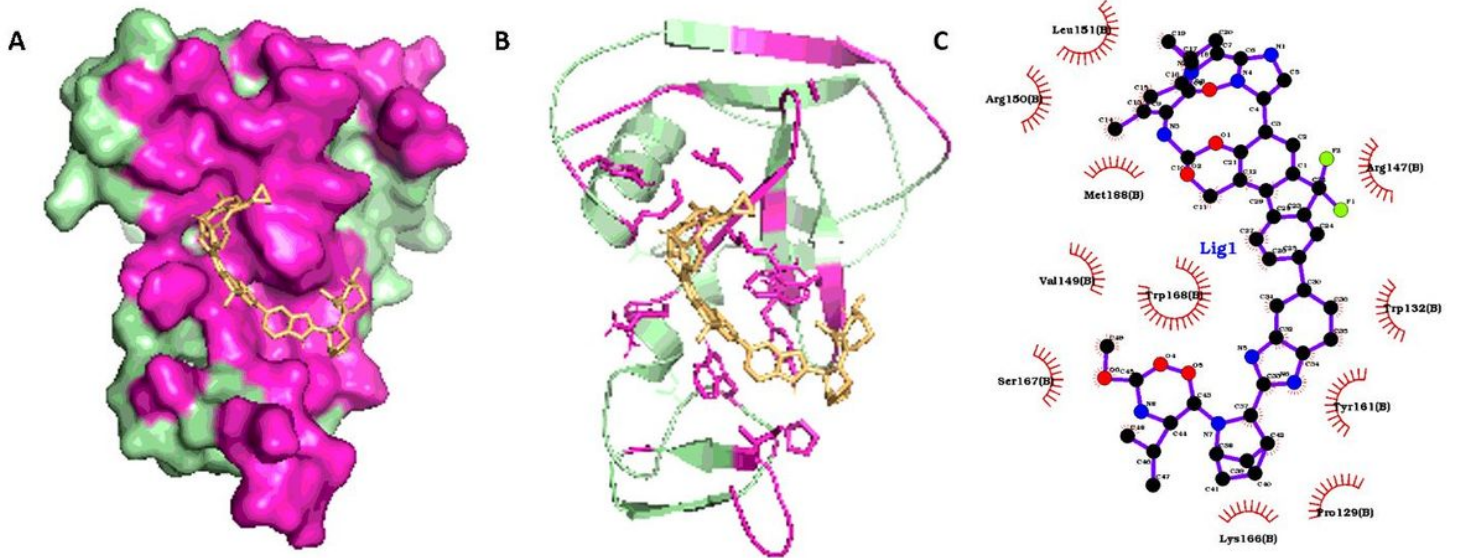


Figure 5

Binding pose of top FDA approved drug(Ledipasvir) binding to hNECD blocking VS2'. Panel A and B shows Ledipasvir binding to hNECD with interface residues represented in magenta color. Panel C shows residue level interaction of Ledipasvir with hNECD generated using LigPlot+ (Laskowski and Swindells, 2011). Panel A and B were generated using PyMol (Schrodinger, LLC).

Figure 6

Binding pose of phytochemical compound (Isoarbooreol) binding to hNECD blocking VS2'. Panel A and B shows Isoarbooreol binding to hNECD with interface residues represented in magenta color. Panel C shows residue level interaction of Isoarbooreol with hNECD generated using LigPlot+ (Laskowski and Swindells, 2011). Panel A and B were generated using PyMol (Schrodinger, LLC).

Supplementary Files

This is a list of supplementary files associated with this preprint. Click to download.

- [SupplementaryData.docx](#)